ELSEVIER

Journal of Atmospheric and Solar-Terrestrial Physics 67 (2005) 1269–1279

Journal of ATMOSPHERIC AND SOLAR-TERRESTRIAL PHYSICS

www.elsevier.com/locate/jastp

Strong DC electric field formation in the low latitude ionosphere over typhoons

V.M. Sorokin[a,*], N.V. Isaev[a], A.K. Yaschenko[a], V.M. Chmyrev[b], M. Hayakawa[c]

[a]*Institute of Terrestrial Magnetism, Ionosphere and Radio Wave Propagation (IZMIRAN), Russian Academy of Sciences, Troitsk, Moscow Region, Russia*

[b]*Institute of the Earth Physics, Russian Academy of Sciences, Moscow, Russia*

[c]*Department of Electronic Engineering, The University of Electro-Communications, Tokyo, Japan*

Received 25 May 2004; received in revised form 6 June 2005; accepted 22 June 2005
Available online 10 August 2005

Abstract

This paper presents further development of the electrodynamic model of strong electric field formation in the ionosphere above the regions of tropical storm and typhoon origin and its comparison with new experimental results obtained from the satellite observations of DC electric field and plasma density variations over such regions. According to this model the electric field disturbance arises due to perturbation in the atmosphere–ionosphere electric circuit generated by the upward transport of charged water drops and aerosols in the hurricane convection zone. Calculations of spatial distribution of DC electric field in the ionosphere were carried out with the account of oblique geomagnetic field and the conjugate ionosphere effects. Direct measurements onboard the COSMOS-1809 satellite revealed localized DC electric field disturbances with magnitudes up to 25 mV/m and accompanying plasma density variations $\delta n/n \sim 6\%$ over the zones of strong atmospheric perturbations. Comparison of observational data with the results of theoretical modeling shows that the considered model adequately describes the electrodynamic impact of meteorological processes on the ionosphere.

Keywords: Ionosphere; Typhoon; Electric field; External current; Convective transport

1. Introduction

Response of the ionosphere and the upper atmosphere to intense meteorological processes was studied by Kelley (1989); Kelley et al. (1985) and Holzworth et al. (1985) who have made measurements of the electric field over active thunderstorm clouds. A DC electric field exceeding 80 mV/m in magnitude was observed in the stratosphere at distances ~100 km from thunderstorm cells. Besides AC electric fields with amplitude above 10 mV/m and significant magnetic field-aligned component were registered in the ionosphere. Electric conductivity at altitudes 30–70 km appeared to be much lower then it was usually considered at the theoretical modeling. It was found that the vertical electric current density exceeded 120 pA/m^2 at altitudes 50–60 km. Burke et al. (1992) reported the observations of AC electric fields ~40 mV/m and correlated intensity bursts of upward magnetic field-aligned fluxes of 1 keV electrons over hurricane Debby. Mikhailova et al. (2000) discussed the satellite observations of ULF/VLF emissions possibly connected with hurricane

*Corresponding author. Tel.: +7 095 330 9902; fax: 7 095 334 0124.
E-mail address: sova@izmiran.ru (V.M. Sorokin).

1364-6826/$ - see front matter © 2005 Elsevier Ltd. All rights reserved.
doi:10.1016/j.jastp.2005.06.014

development. Data on DC electric fields with magnitudes up to 20 mV/m observed in the upper ionosphere over the tropical cyclone zone were presented by Isaev et al. (2002a, b). It is important to note that the above mentioned phenomena have many properties typical for the disturbances of seismic origin. Among them are anomalous DC electric fields, ULF/ELF electromagnetic emissions (Gokhberg et al., 1982; Chmyrev et al., 1989; Bilichenko et al., 1990; Serebryakova et al., 1992; Molchanov et al., 1993; Parrot, 1994) and plasma density inhomogeneities (Chmyrev et al., 1997; Afonin et al., 1999) observed in the ionosphere prior to strong earthquakes. One of the most developed interpretations of these phenomena is based on the atmosphere–ionosphere coupling provided by the effects of DC electric field generation (Sorokin et al., 1998, 2000, 2001; Sorokin and Cherny, 1999; Sorokin and Yaschenko, 2000; Borisov et al., 2001). Calculation of the electric field in the ionosphere over thunderstorm clouds was carried out by Park and Dejnakarintra (1973). Mechanism of DC electric field formation in the ionosphere in a process of typhoon development was discussed by Sorokin and Cherny (1999) and Isaev et al. (2002b). The general idea of this mechanism is as follows. The electro-physical parameters of the lower troposphere such as concentration, dimensions and mobility of charge marine aerosols and dielectric constant of air are correlated with the meteorological parameters—cloudiness, temperature, humidity, pressure and intensity of atmospheric convection. Perturbations in the meteorological parameters at definite phases of tropical cyclone development initiate the disturbances of electrical conductivity that leads to formation of external electric current in the lower atmosphere. This current arises as result of vertical atmospheric convection and related transport of charged water drops and aerosols. Insertion of external electric current modifies the distribution of conductivity current in global atmosphere–ionosphere electric circuit and leads to generation of DC electric field disturbances over a zone of strong atmospheric perturbation. The most important property of this mechanism is that numerous electromagnetic and plasma effects can be explained by the operation of only one source—an amplification of DC electric field in the ionosphere. This source is controlled by the dynamics of atmospheric processes through modification of electrical parameters of the lower atmosphere.

This paper presents further development of the above mechanism taking into account the oblique geomagnetic field and the conjugate ionosphere effects. Results of theoretical modeling are compared with new experimental data obtained from electromagnetic and plasma measurements onboard the COSMOS-1809 satellite and meteorological observations of strong tropical storms and typhoons.

2. Derivation of the equation for electric field potential

Let us consider the formation of spatial distribution of the conductivity current and related electric field in the conductive atmosphere and the ionosphere by external current $\mathbf{j}_e$ located in the lower atmosphere. To do it we derive the set of equations for potential φ of the electric field disturbance $\mathbf{E} = -\nabla\varphi$. The Cartesian coordinate system $(x, y, z)$with the z-axis directed vertically upward and x-axis lying in the plane of magnetic meridian is used. Homogeneous magnetic filed is assumed to be directed at the angle α to x-axis. The plane $z = 0$ coincides with the surface of ideally conducted ground. We assume that on this plane the electric field potential is zero ($\varphi|_{z=0} = 0$) and the atmosphere with the altitude-dependent conductivity $\sigma(z)$ lies in the layer $0 < z < z_1$. Potential φ in this layer is determined from the current continuity equation and Ohm's law:

$$\nabla(\mathbf{j} + \mathbf{j}_e) = 0, \quad \mathbf{j} = \sigma\mathbf{E} = -\sigma\nabla\varphi,$$

from which the equation for potential can be found:

$$\frac{\partial^2\varphi}{\partial z^2} + \frac{1}{\sigma(z)}\frac{\mathrm{d}\sigma(z)}{\mathrm{d}z}\frac{\partial\varphi}{\partial z} + \Delta_\perp\varphi = \frac{1}{\sigma(z)}\nabla\mathbf{j}_e. \tag{1}$$

Plane $z = z_1$ coincides with thin conductive ionosphere characterized by the tensor integral conductivity Σ. The boundary condition for potential on the ionosphere can be obtained by integrating the current continuity equation $\nabla \cdot \mathbf{j} = 0$ along the geomagnetic field line within the ionospheric layer. Its derivation is given in Appendix A. In approximation of thin ionosphere, large horizontal scale of external current and not too small angle α the boundary condition has a form (see Eq. (A.8)):

$$j_z(z_1 + 0) - j_z(z_1 - 0) = \Sigma_P\left(\frac{1}{\sin^2\alpha}\frac{\partial^2\varphi_1}{\partial x^2} + \frac{\partial^2\varphi_1}{\partial y^2}\right), \tag{2}$$

where $\varphi_1 = \varphi(z_1)$ and Σ_P is the Pedersen integral conductivity of the ionosphere. For vertical magnetic field ($\alpha = \pi/2$) Eq. (2) coincides with the condition obtained by Isaev et al. (2002b). In quasi-static approximation geomagnetic field lines are equipotential. Therefore the distribution of electrical potential of the ionosphere and the field-aligned current on its upper boundary are transported into the magnetically conjugate region without changes. Magnetic field-aligned electric current flowing in the magnetosphere is closed by transverse conductivity current in the conjugate ionosphere and the atmosphere. The boundary condition on the conjugate ionosphere is similar to Eq. (2) and the equation for potential in the conjugate atmosphere coincides with Eq. (1) at $\mathbf{j}_e = 0$. Let us take the altitude dependence of atmospheric conductivity in a form:

$$\sigma(z) = \sigma_0 \exp(z/h), \tag{3}$$

where h is the spatial scale of atmospheric conductivity. We will assume that external current has only vertical component $j_{ez} = j_e(z, \mathbf{r})$ where radius vector $\mathbf{r}$ lies in the plane (x, y). Applying the Fourier transform

$$\Phi(\mathbf{k}, z) = \int_{-\infty}^{\infty}\int_{-\infty}^{\infty} \varphi(\mathbf{r}, z)\exp(-i\mathbf{k}\cdot\mathbf{r})\,\mathrm{d}\mathbf{r},$$

to Eq. (1) and boundary condition (2) gives

$$\begin{aligned}
&\frac{\mathrm{d}^2\Phi}{\mathrm{d}z^2} + \frac{1}{h}\frac{\mathrm{d}\Phi}{\mathrm{d}z} - k^2\Phi = \frac{1}{\sigma}\frac{\mathrm{d}j_e}{\mathrm{d}z}, \quad 0 < z < z_1,\\
&\Phi|_{z=0} = 0, \quad j_m \sin\alpha + \sigma_1 \left.\frac{\mathrm{d}\Phi}{\mathrm{d}z}\right|_{z=z_1-0}\\
&\quad = -\Sigma_P\left(\frac{k_x^2}{\sin^2\alpha} + k_y^2\right)\Phi_1,\\
&k = \sqrt{k_x^2 + k_y^2}, \quad \Phi_1 = \Phi(z_1),
\end{aligned} \tag{4}$$

where j_m is field-aligned current in the magnetosphere. Let z' denote the upward directed vertical axis of the Cartesian co-ordinate system in the conjugate atmosphere. The equation for potential and the boundary conditions in this region are as follows:

$$\begin{aligned}
&\frac{\mathrm{d}^2\Phi}{\mathrm{d}z'^2} + \frac{1}{h}\frac{\mathrm{d}\Phi}{\mathrm{d}z'} - k^2\Phi = 0, \quad 0 < z' < z_1,\\
&\Phi|_{z'=0} = 0, \quad -j_m \sin\alpha + \sigma_1 \left.\frac{\mathrm{d}\Phi}{\mathrm{d}z'}\right|_{z'=z_1-0},\\
&= -\Sigma_P\left(\frac{k_x^2}{\sin^2\alpha} + k_y^2\right)\Phi_1.
\end{aligned} \tag{5}$$

The solution of Eq. (5) in the conjugate atmosphere satisfying the boundary condition on the Earth surface has a form

$$\Phi = \Phi_1 \exp\left[-\frac{z' - z_1}{2h}\right]\frac{\sinh(qz')}{\sinh(qz_1)}, \quad q = \sqrt{k^2 + \frac{1}{4h^2}}.$$

Substitution of this solution in the boundary condition (5) gives field-aligned electric current in the magnetosphere:

$$\begin{aligned}
&j_m = \left[\Sigma_P\left(k_x^2/\sin^2\alpha + k_y^2\right) + \sigma_1(q\coth(qz_1) - 1/2h)\right]\\
&\Phi_1/\sin\alpha, \quad \sigma_1 = \sigma(z_1).
\end{aligned}$$

Using this expression in Eq. (4) yields the boundary condition for the electric field potential on the lower edge of the ionosphere. A following set of equations and the boundary conditions allows the calculation of spatial distribution of the electric field connected with the appearance of external current in the Earth–ionosphere electric circuit with account of conjugate ionosphere:

$$\begin{aligned}
&\frac{\mathrm{d}^2\Phi}{\mathrm{d}z^2} + \frac{1}{h}\frac{\mathrm{d}\Phi}{\mathrm{d}z} - k^2\Phi = \frac{1}{\sigma}\frac{\mathrm{d}j_e}{\mathrm{d}z},\\
&\varphi(\mathbf{r}, z) = \int_{-\infty}^{\infty}\int_{-\infty}^{\infty}\Phi(\mathbf{k}, z)\exp(i\mathbf{k}\cdot\mathbf{r})\frac{\mathrm{d}\mathbf{k}}{(2\pi)^2},\\
&\Phi|_{z=0} = 0; \quad \left[\frac{\mathrm{d}\Phi}{\mathrm{d}z} + a(\mathbf{k})\Phi\right]_{z=z_1-0} = 0,\\
&a(\mathbf{k}) = \frac{2\Sigma_P}{\sigma_1}\left(\frac{k_x^2}{\sin^2\alpha} + k_y^2\right) + q\coth(qz_1) - \frac{1}{2h}.
\end{aligned} \tag{6}$$

Influence of conjugate region on the field distribution in the atmosphere is accounted by the boundary condition in Eq. (6).

3. Approximate method for the field computation

The external current formation processes over the region of tropical cyclone are connected with vertical convective motion of gases in the lower atmosphere. These processes cover a zone with horizontal scale l of the order of few hundreds km. At such spatial scale Eq. (1) with boundary condition (2) can be approximately solved for arbitrary dependence of the atmosphere conductivity on altitude. Taking into consideration that in the order of magnitude the last summand in the left part of Eq. (1) is about Φ/l^2 while the first and second summands are $\sim\Phi/h^2$, where h is characteristic spatial scale of altitude variation of the atmosphere conductivity, we can neglect the last item in comparison with first two. As a result, the simplified equation will have a form

$$\frac{\mathrm{d}}{\mathrm{d}z}\left[\sigma(z)\frac{\mathrm{d}\varphi}{\mathrm{d}z} - j_e(z, \mathbf{r})\right] = 0. \tag{7}$$

Let us find the potential boundary conditions on the plane $z = z_1$. Conditions for current continuity in conjugate regions of the ionosphere have a form

$$\begin{aligned}
&j_m \sin\alpha + \sigma_1 \left.\frac{\mathrm{d}\varphi}{\mathrm{d}z}\right|_{z=z_1-0} = \Sigma_P\left(\frac{1}{\sin^2\alpha}\frac{\partial^2\varphi_1}{\partial x^2} + \frac{\partial^2\varphi_1}{\partial y^2}\right),\\
&-j_m \sin\alpha + \sigma_1 \left.\frac{\mathrm{d}\varphi}{\mathrm{d}z}\right|_{z'=z_1-0} = \Sigma_P\left(\frac{1}{\sin^2\alpha}\frac{\partial^2\varphi_1}{\partial x^2} + \frac{\partial^2\varphi_1}{\partial y^2}\right).
\end{aligned} \tag{8}$$

The solution of Eq. (7) at $j_e = 0$ in the conjugate atmosphere yields

$$\sigma_1 \left.\frac{\mathrm{d}\varphi}{\mathrm{d}z}\right|_{z'=z_1-0} = \frac{\varphi_1}{\rho}, \quad \rho = \int_0^{z_1}\frac{\mathrm{d}z}{\sigma(z)}. \tag{9}$$

From substitution of Eq. (9) in the second Eq. (8) and summation of two Eqs. (8) we find the boundary

condition on the ionosphere for Eq. (7):

$$\varphi|_{z=0}=0,\quad \sigma_1\left.\frac{\mathrm{d}\varphi}{\mathrm{d}z}\right|_{z=z_1-0} = 2\Sigma_P\left(\frac{1}{\sin^2\alpha}\frac{\partial^2\varphi_1}{\partial x^2}+\frac{\partial^2\varphi_1}{\partial y^2}\right)-\frac{\varphi_1}{\rho}. \tag{10}$$

Boundary condition (10) takes into account transverse spreading of current in the ionosphere at $z\geqslant z_1$. This conductivity current determines the horizontal component of the electric field in the ionosphere. Solution of Eq. (7) satisfying the condition $\varphi|_{z=0}=0$ has a form

$$\varphi(\mathbf{r},z)=\int_0^z\frac{j_e(\mathbf{r},z')}{\sigma(z')}\mathrm{d}z'-j_1(\mathbf{r})\int_0^z\frac{\mathrm{d}z'}{\sigma(z')},$$
$$j_1(\mathbf{r})=\frac{\varepsilon(\mathbf{r})-\varphi_1(\mathbf{r})}{\rho},\quad \varepsilon(\mathbf{r})=\int_0^{z_1}\frac{j_e(\mathbf{r},z)}{\sigma(z)}\,\mathrm{d}z. \tag{11}$$

In this equation $j_1(\mathbf{r})$ is a density of electric current on the lower ionospheric boundary. This current flows into the ionosphere from the atmosphere. Values ε and ρ mean the electromotive force of external current and the electrical resistance of a unitary area column in the layer between the Earth and the ionosphere. Using Eq. (11) the boundary condition (10) yields the equation for horizontal distribution of the ionosphere potential φ_1:

$$\left(\frac{1}{\sin^2\alpha}\frac{\partial^2\varphi_1}{\partial x^2}+\frac{\partial^2\varphi_1}{\partial y^2}\right)-\frac{1}{2\Sigma_P\rho}\varphi_1(\mathbf{r})=-\frac{j_1(\mathbf{r})}{2\Sigma_P}.$$

Estimates show that when $l\ll 10^8$ m (that is true practically in all cases) the second term in the left part of this equation is negligibly small. Therefore this equation can be reduced to the following form:

$$\frac{1}{\sin^2\alpha}\frac{\partial^2\varphi_1}{\partial x^2}+\frac{\partial^2\varphi_1}{\partial y^2}=-\frac{j_1(\mathbf{r})}{2\Sigma_P}. \tag{12}$$

At $\alpha=\pi/2$ this expression coincides with 2D Poisson equation. Slope of geomagnetic field effects on a spatial scale of the ionosphere potential distribution in meridional direction. Eqs. (11) and (12) are applicable for calculation of the electric fields induced by external currents with arbitrary distribution in horizontal plane and for any altitude dependence of the atmosphere electric conductivity in all cases when characteristic horizontal scale of currents exceeds the height of lower boundary of the ionosphere. To check an accuracy of approximate calculation method we carried out comparison of solutions (11) of Eq. (7) with exact solutions obtained from full set of Eqs. (6) for the model distribution of atmospheric conductivity (3). Comparison was made for the case of vertical magnetic field $\alpha=\pi/2$. An altitude distribution of external current was taken in exponential form and the horizontal distribution—in a form of axially symmetric Gauss function. It was found that the maximum inaccuracy of approximate method is 22, 7 and 3 percents for the horizontal scales of external current ~100, 200 and 300 km, correspondingly. Thus the suggested method for approximate calculations provides acceptable accuracy in the events of large enough horizontal size of external current exceeding a height of the lower ionosphere.

4. Computation of the electric field magnitude in the ionosphere

Let us choose large-scale axial symmetric distribution of external current in the form

$$j_e(r,z)=j_{e0}\exp\left(-\frac{z}{h_j}\right)\exp\left(-\frac{x^2+y^2}{l^2}\right), \tag{13}$$

where j_{e0} is the magnitude of external current near the Earth surface, h_j, l are the vertical and horizontal scales of external current. According to Eqs. (11) and (12) distribution (13) leads to following equation for the ionosphere potential:

$$\frac{1}{\sin^2\alpha}\frac{\partial^2\varphi_1}{\partial x^2}+\frac{\partial^2\varphi_1}{\partial y^2}=-A\exp\left(-\frac{x^2+y^2}{l^2}\right), \tag{14}$$

where

$$A=\frac{j_{e0}}{2\Sigma_P}\int_0^{z_1}\frac{\exp(-z/h_j)}{\sigma(z)}\,\mathrm{d}z\Big/\int_0^{z_1}\frac{\mathrm{d}z}{\sigma(z)}.$$

Using the atmosphere conductivity in form (3) yields

$$A=j_{e0}h_j/2\Sigma_P(h+h_j). \tag{15}$$

Let us introduce the dimensionless derivatives in Eq. (14):

$$\xi=x/l,\quad \eta=y/l,\quad \psi=-\varphi_1/Al^2,$$

where ψ is determined from the equation:

$$\frac{1}{\sin^2\alpha}\frac{\partial^2\psi}{\partial\xi^2}+\frac{\partial^2\psi}{\partial\eta^2}=\exp(-\xi^2-\eta^2).$$

Application of Fourier transforms $\tilde{\psi}(s,\eta)=\int_{-\infty}^{\infty}\psi(\xi,\eta)\exp(-is\xi)\,\mathrm{d}\xi$ to this equation yields

$$\frac{\mathrm{d}^2\tilde{\psi}}{\mathrm{d}\eta^2}-\frac{s^2}{\sin^2\alpha}\tilde{\psi}=\sqrt{\pi}\exp\left(-\frac{s^2}{4}-\eta^2\right).$$

The solution of this equation diminishing at $|\xi|\to\infty$ has a form

$$\tilde{\psi}(s,\eta)=-\frac{\pi\sin\alpha}{|s|}[g(\eta,s)+g(-\eta,s)],$$
$$g(s,\eta)=\frac{1}{4}\exp\left(\frac{s^2}{4\tan^2\alpha}+\frac{|s|\eta}{\sin\alpha}\right)\mathrm{Erfc}\left(\frac{|s|}{2\sin\alpha}+\eta\right). \tag{16}$$

Spatial structure of dimensionless potential is determined by Fourier inversion of Eq. (16). Horizontal distribution of the electric field components in the

ionosphere is described by the following expressions:

$$E_x = E_0 \sin\alpha \int_0^\infty \sin(s\xi)[g(\eta,s)+g(-\eta,s)]\,\mathrm{d}s,$$
$$E_y = -E_0 \int_0^\infty \cos(s\xi)[g(\eta,s)-g(-\eta,s)]\,\mathrm{d}s,$$
$$E_z = -E_y/\tan\alpha; \quad E_0 = j_{e0}h_j l/2\Sigma_P(h+h_j). \tag{17}$$

Graphs of horizontal component $E_r(r,\varphi) = \sqrt{E_x^2+E_y^2}$ of the electric field in the ionosphere calculated from Eq. (17) for different angles $\varphi = \arctan(y/x)$ are presented in Fig. 1. Note that $r = \sqrt{x^2+y^2}$, angle $\varphi = 0$ corresponds to plane of magnetic meridian and $\varphi = \pi/2$ to transverse direction. For calculations we used the magnitude of external current obtained by Isaev et al. (2002b). External current can be induced by vertical atmospheric convection acting as electrostatic generator. Upward airflow transports small positively charged particles, while downward precipitations transfer negative charge. A rate of charge separation in unitary volume of cloud is of the order of $\mathrm{d}Q/\mathrm{d}t = 1\ \mathrm{C/km^3\,min} \sim 10^{-11}\,\mathrm{C/m^3\,s}$. Apparently, the vertical convective motion of moist atmosphere at upper altitudes in typhoon zone is characterized by lower separation rates, which are not known exactly. We assume that at the heights $z_0 = 10\,\mathrm{km}$ an average charge separation rate is $\sim 4\times10^{-12}\,\mathrm{C/m^3\,s}$. In this case the estimate yields $j_{e0}\sim(\mathrm{d}Q/\mathrm{d}t)z_0 \sim 4\times10^{-6}\,\mathrm{A/m^2}$. Graphs in Fig. 1 are calculated at the following parameters: $l = 100$, $h = 5$, $h_j = 10\,\mathrm{km}$, $\Sigma_P = 10^{12}\,\mathrm{cm/s}$, $\alpha = 20°$. It is seen from Fig. 1 that the electric field component lying in the plane of magnetic meridian is substantially lower then the perpendicular one. Fig. 2 presents the horizontal distribution of radial component of the electric field E_r calculated from Eq. (17) for the same set of the parameters at different magnetic field inclinations (α). It is seen that the distribution strongly depends on α. The field structure becomes two-cell (dipole-like) with very small component in the plane of meridian (in a center of hurricane) when inclination decreases below 20°.

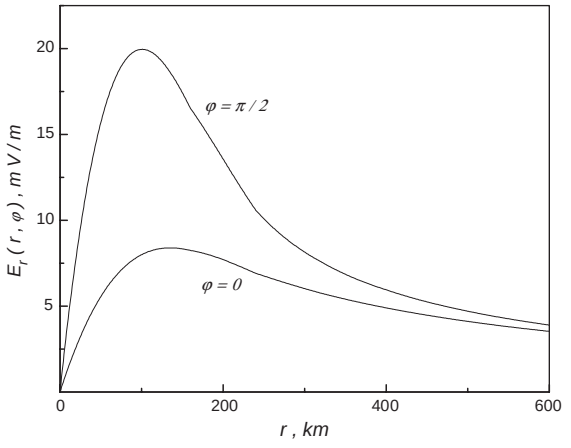

Fig. 1. Dependence of radial electric field component on distances along and across the plane of magnetic meridian.

5. Comparison with the satellite observations

For verification of the above presented theoretical model of hurricane effects on the ionosphere we have analyzed the data on DC electric field and plasma density measurements made onboard the COSMOS-1809 satellite at the passages over tropical cyclone regions at the altitudes ~950 km. Description of instruments and data reduction methodology is given in Isaev et al. (2002a, b). Accuracy and range of DC electric field measurements were ±0.5 and ±500 mV/m, correspondingly. The spatial resolution was ~20 km for the electric field (E_x and E_y) and plasma density (N_e) measurements and ~4 km for plasma density variations $\mathrm{d}N_e$. The data are presented in satellite co-ordinate system with the x-axis directed along the satellite velocity, z-axis directed vertically upward and y-axisaccomplishing the right-hand coordinates. Since the inclination of satellite orbit was 83° the orientation of E_x and E_y at the low latitudes and near the equator was approximately in the North–South and East–West directions, correspondingly.

Fig. 3 presents an example of records of two electric field components (E_x and E_y), plasma density (N_e) and plasma density variations $\mathrm{d}N_e$ made onboard the COSMOS-1809 at three passages over the zone of typhoon HARRY on 10 and 13 February 1989. This typhoon was observed in the South-West part of the Pacific Ocean from 7 to 19 February 1989. Co-ordinates of the typhoon center during the satellite passage on 10 February were −20.5°S and 161°E. The vertical arrow in Fig. 3a indicates a moment when satellite passed at minimal distance ~1.5° eastward of the typhoon center. These records were made in night sector of local time in the conditions of moderate geomagnetic activity ($K_p = 3_+$). As seen from Fig. 3a the electric field disturbance with magnitude up to 15 mV/m in y-component was observed in the longitude range from 162.3° to 162.7°, that was ~1.5° eastward from the center of atmospheric perturbation. Shift in latitudes between the electric field amplification zone ($-13° < \phi < -19.50$) and the typhoon area corresponds to conjugate matching along equipotential geomagnetic field lines from the dynamo-region of the ionosphere to the satellite heights. Fig. 3b presents the results of similar measurements carried out at the large distance ~12 000 km in longitude from the typhoon center (it was at −19°S and 165°E) during the same day about 7 h before the event considered above. The observation conditions were practically the same with respect to

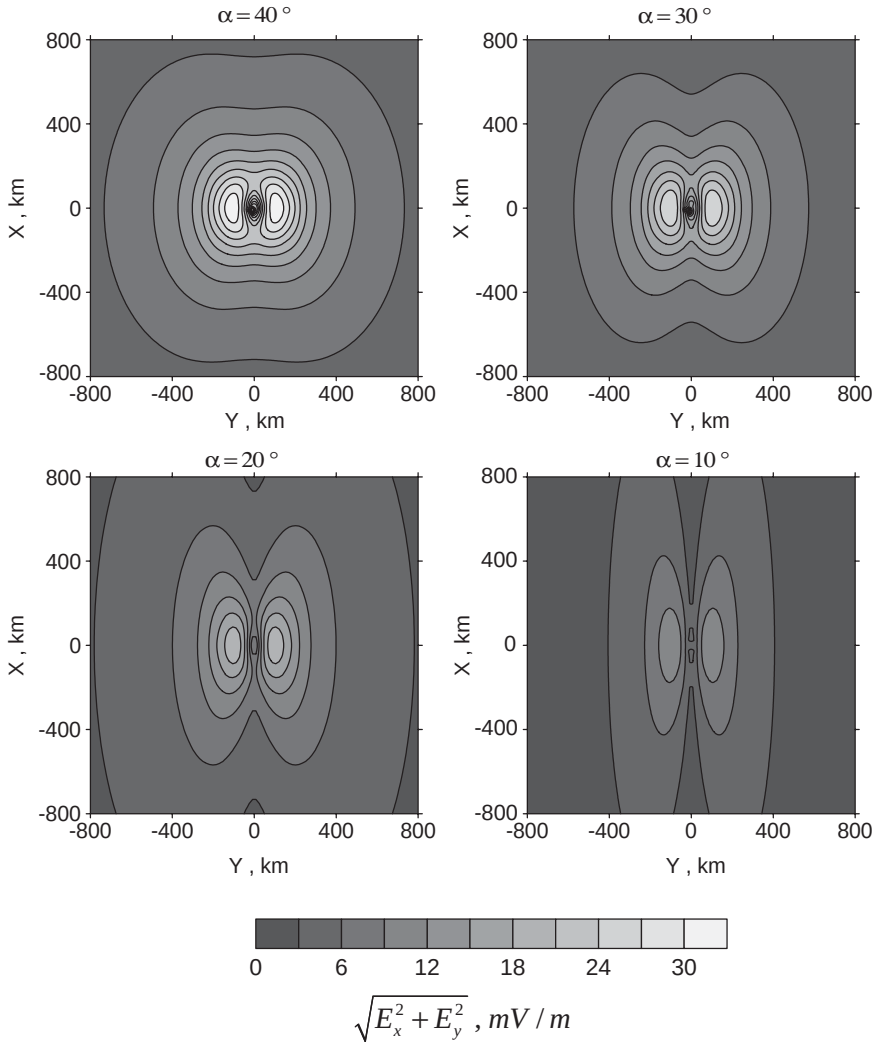

Fig. 2. Spatial distribution of horizontal electric field component in the ionosphere over typhoon calculated for different magnetic field inclinations.

satellite shadowiness and geomagnetic activity ($K_p = 3$). It is seen from Fig. 3b that neither electric field nor plasma density disturbances were observed at this passage in vicinity of the typhoon latitudes. Variations of plasma density dN_e in this event are typical for low latitude ionosphere. The third event shown in Fig. 3c is related to observations over the same typhoon approximately 3 days after the first one presented in Fig. 3a. In this case the satellite passed about 10° eastward from the typhoon center, which was in the region with co-ordinates: $\lambda = 159°$S, $\phi = 19.3°$E. The magnitude of the electric field disturbance in this event was 7–8 mV/m. Analogous results of the satellite measurements were obtained for few other similar meteorological phenomena in the Indian Ocean. Fig. 4 presents another example of the satellite records made over the region of a strong tropical storm EDME that occurred 19–28 January 1989 in the south part of Indian Ocean. Geographic co-ordinates of storm epicenter in this event were: −34°S and 71.5°E. The electric field disturbance ~12 mV/m was observed in the area connected with the storm region along geomagnetic field lines as in Fig. 3b and c.

Figs. 3 and 4 show that the electric field disturbances are accompanied by enhancement of plasma density up to 20% with regard to background values and appearance of small-scale fluctuations of plasma density with relative magnitude dN_e/N_e ~8%. We assume that such fluctuations in satellite records arise when satellite crosses magnetic field-aligned plasma density irregularities. To estimate characteristic spatial scale of these irregularities we carried out spectral analysis using the

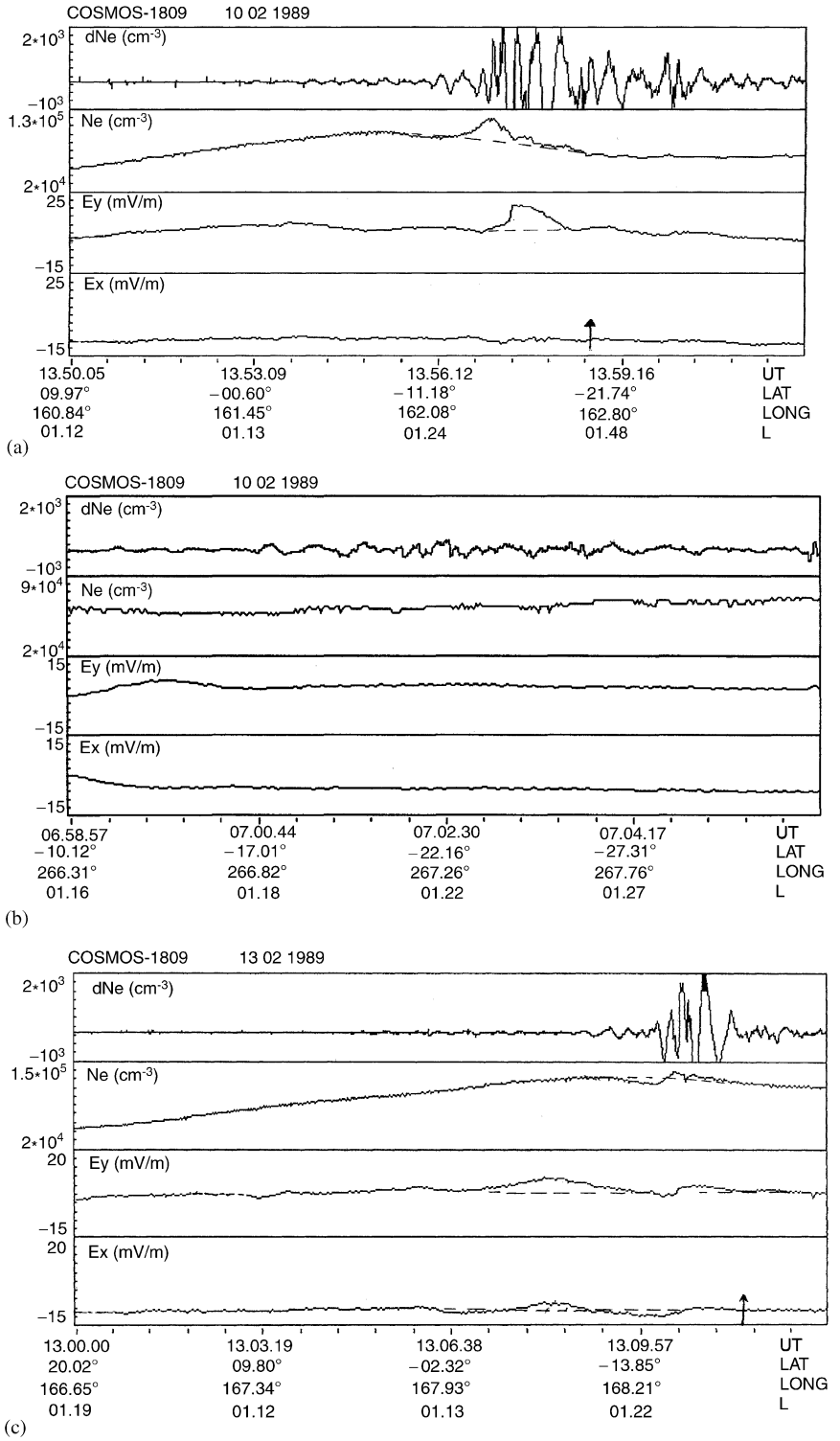

Fig. 3. Horizontal components of DC electric field (E_x and E_y), electron density N_e and its variations dN_e as observed onboard the COSMOS-1809 satellite over typhoon HARRY (a and b) and in a distance of it (c). An arrow in panels a and c indicates the moment when the satellite was at the minimal distance from the typhoon center.

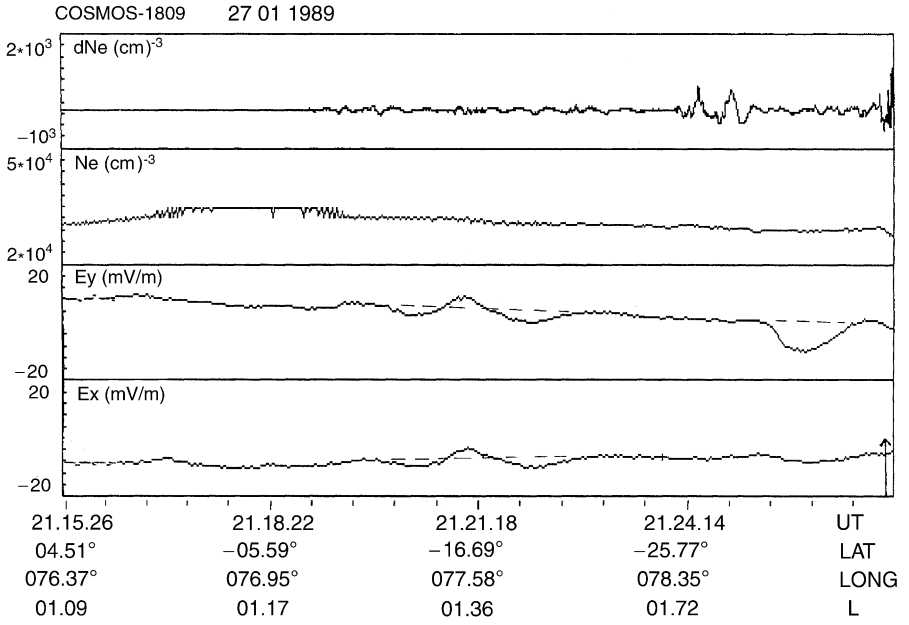

Fig. 4. The same parameters observed onboard the COSMOS-1809 satellite over the zone of strong tropical storm EDME occurred 19–28 January 1989 in the south part of the Indian Ocean.

same technique as in Phelps and Sagalyn (1976). Each sample contains $N = 2996$ individual measurements. The time interval δ between successive measurements is 0.256 s. The power spectrum $S(f)$ of the electron density irregularity distribution in the spectral range $|f| < 1/2\delta = 1.95$ Hz is obtained by Fourier transforming the normalized autocorrelation function ρ:

$$S(f) = \delta \sum_{L=-(M-1)}^{M-1} W(L)\rho(L)\exp(-\mathrm{i}2\pi fL\delta),$$

$$\rho(L) = \frac{(1/N)\sum_{I=1}^{N-L}[\Delta n(I)][\Delta n(I+L)]}{(1/N)\sum_{I=1}^{N-L}[\Delta n(I)]^2},$$

where $\Delta n(I)$ is the deviation of the Ith measurement:

$$\Delta n(I) = n(I) - \frac{1}{N}\sum_{I=1}^{N} n(I)$$

and $W(L)$ is the Tukey lag window:

$$W(L) = \begin{cases} [1+\cos(\pi L/M)]/2, & L \leqslant M \\ 0, & L > M \end{cases}.$$

Number of lags, was chosen as $M = 400$. Fig. 5 presents the power spectra calculated for the temporal dependences of plasma density fluctuations given in Fig. 3 and 4. The calculations show that in the event of 27 January 1989 there were two maximums in spectra at the frequencies 0.04 and 0.07 Hz (corresponding periods 25 and 14 s). At the satellite velocity ~8 km/s it gives the spatial scale of irregularities along the orbit ~200 and 110 km. To estimate their transverse scale it is necessary

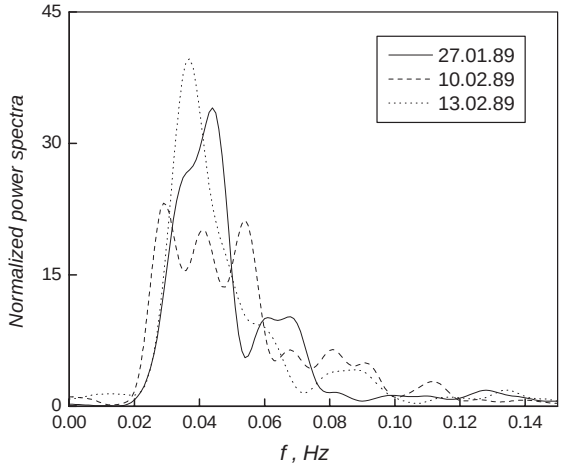

Fig. 5. Normalized power spectra of electron density fluctuations shown in Figs. 3 and 4.

to multiply these values by sin α, where α is an angle between the vectors of satellite velocity and geomagnetic field. At the low latitude α is about 5–10°. Therefore the characteristic size of irregularities across geomagnetic field is 20–40 km and 10–20 km in the considered case. Similar results are obtained for the event of 13 February 1989. At the passage closest to the typhoon center (10 February 1989, Fig. 3a) there were three maximums near the frequency 0.04 Hz.

Generation mechanism of plasma irregularities caused by DC electric field amplification in the ionosphere was

suggested by Sorokin et al.(1998). This mechanism is based on the instability of acoustic-gravity waves, forming horizontal inhomogeneities of electrical conductivity, magnetic field-aligned currents and related plasma density irregularities stretched along geomagnetic field lines. Irregularities of such kinds were observed earlier in the ionosphere over earthquake preparation zone (Chmyrev et al., 1997).

Let us consider the possible sources of observed DC electric field disturbances in the low latitude ionosphere. It is known that the auroral electric fields do not penetrate to the latitudes below 45–40°. The low latitude electric field magnitude arising due to dynamo effect normally does not exceed ~1 mV/m (Isaev et al., 1987). The upward directed polarization field connected with equatorial electro jet is usually less then 1–2 mV/m. Specifically, it was shown in a series of rocket measurements in E and F regions of the ionosphere conducted by Raghavarao et al. (1987). The electric field magnitudes given in Figs. 3 and 4 substantially exceed typical low latitude electric fields in the ionosphere. Therefore we can assume that they are not connected with any sources located in the ionosphere and the magnetosphere. The facts that these fields were observed over typhoon regions and that the character of records was similar for different typhoons gives the ground to suppose that the disturbances of DC electric field and plasma density presented in Figs. 3 and 4 were connected with the development of strong large-scale atmospheric perturbations.

The special analysis was carried out to avoid possible "technical" effects that could be connected with geomagnetic or solar shadowing of electric field sensors onboard the satellite as well as the influence of terminator.

6. Conclusion

Convective transport of charged aerosols in the lower atmosphere at different stages of typhoon development leads to formation of external electric current. Its inclusion in the atmosphere–ionosphere electric circuit is accompanied by amplification of conductivity current that flows into the ionosphere. The current flowing within the conducted layer of the ionosphere is closed in the conjugate ionosphere through the magnetic field-aligned current. The computation method presented in this paper allows calculating the spatial distribution of the conductivity current and related electric field for arbitrary altitude dependence of atmospheric conductivity and horizontal distribution of external electric current at oblique geomagnetic field. The calculations shown that DC electric field in the ionosphere can reach the magnitudes 10–20 mV/m. The horizontal component lying in the plane of geomagnetic meridian in typhoon center decreases with decreasing magnetic field inclination. Analysis of satellite data revealed the electric field disturbances up to 15 mV/m in the ionosphere over typhoon region. Generation of such fields is accompanied by local growth of plasma density and formation of magnetic field-aligned plasma layers with transverse scales 10–20 and 20–40 km. In the records made onboard the satellite crossing these layers they are seen as plasma density fluctuations.

Acknowledgments

This research was partially supported by ISTC under Research Grant No. 2990, by Russian Fund for Basic Research through the Grant No. 03-05-64553.

Appendix A

Potential of the electric field disturbance in the ionosphere is determined by continuity equation and generalized Ohm's low:

$$\nabla \cdot \mathbf{j} = 0, \quad \mathbf{j} = \widehat{\sigma}\,\mathbf{E} = -\widehat{\sigma}\,\nabla\varphi, \tag{A.1}$$

where $\widehat{\sigma}(z)$ is a tensor of the ionosphere conductivity. We assume that $\widehat{\sigma}(z) \neq 0$ within the layer of widths d and it is zero outside this layer (see Fig. 6). Angle α denotes an inclination of geomagnetic field. Let us turn to the co-ordinates (x', y', z') with the z'-axis directed along geomagnetic field $\boldsymbol{B}$. In these co-ordinates the conductivity tensor has a form

$$\widehat{\sigma} = \begin{pmatrix} \sigma_P & \sigma_H & 0 \\ -\sigma_H & \sigma_P & 0 \\ 0 & 0 & \sigma_\parallel \end{pmatrix}, \tag{A.2}$$

where σ_p and σ_H are Pedersen and Hall conductivities of the ionosphere and $\sigma_\parallel$ is its longitudinal conductivity.

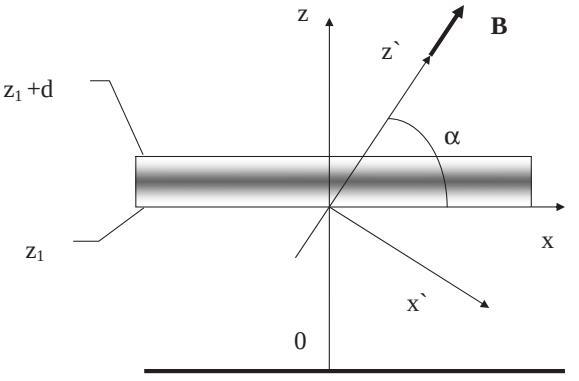

Fig. 6. Scheme and co-ordinate systems used for derivation of the boundary conditions.

Co-ordinates (x', y', z') are connected with (x, y, z) by the following relationships:

$$x' = x \sin\alpha - z\cos\alpha,$$
$$y' = y,$$
$$z' = x\cos\alpha + z\sin\alpha. \quad (A.3)$$

Eq. (A.1) with account of Eq. (A.2) takes the form

$$\frac{\partial}{\partial z'}\left(\sigma_\parallel \frac{\partial\varphi}{\partial z'}\right) + \sigma_P(z)\Delta'_\perp\varphi - \frac{d\sigma_P}{dz}\cos\alpha\frac{d\varphi}{dx'} + \frac{d\sigma_H}{dz}\cos\alpha\frac{d\varphi}{dy'} = 0, \quad z = z'\sin\alpha - x'\cos\alpha, \quad (A.4)$$

where $\Delta'_\perp$ is the Laplace operator on co-ordinates (x', y'). In the ionosphere $\sigma_\parallel \gg \sigma_P, \sigma_H$. Assuming $\sigma_\parallel \to \infty$ in Eq. (A.4) yields the equations:

$$\frac{\partial\varphi}{\partial z'} = 0, \quad \frac{\partial j_\parallel}{\partial z'} = \sigma_P(z)\Delta'_\perp\varphi - \frac{d\sigma_P}{dz}\cos\alpha\frac{d\varphi}{dx'} + \frac{d\sigma_H}{dz}\cos\alpha\frac{d\varphi}{dy'} z = z'\sin\alpha - x'\cos\alpha, \quad (A.5)$$

where $j_\parallel$ is a field-aligned current. First Eq. (A.5) is a condition of geomagnetic field lines equipotentiality. Second equation describes variations of field-aligned current with consideration of conductivity current in a plane of the ionosphere. Let us integrate this equation along geomagnetic field line between the lower edge of the ionosphere ($z = z_1$, $z' = z_1 + x\cos\alpha$) and its upper boundary ($z = z_1 + d, z' = z_1 + d\sin\alpha + x\cos\alpha$) at fixed x' and y'. Note that potential φ does not depend on z'. Since $\sigma_P = \sigma_H = 0$ on the lower and upper boundaries of the ionosphere second Eq. (A.5) yields

$$j_\parallel(z_1 + d\sin\alpha + x\cos\alpha) - j_\parallel(z_1 + x\cos\alpha) = \Delta'_\perp\varphi\int_0^d \sigma_P(z)\frac{dz'}{dz}dz, \quad \frac{dz'}{dz} = \frac{1}{\sin\alpha}. \quad (A.6)$$

Eq. (A.6) written in (x, y, z) co-ordinates has the form

$$j_\parallel(x + d\cot\alpha, y, z_1 + d) - j_\parallel(x, y, z_1) = \frac{\Sigma_P}{\sin\alpha}\left(\frac{1}{\sin^2\alpha}\frac{\partial^2\varphi}{\partial x^2} + \frac{\partial^2\varphi}{\partial y^2}\right), \quad (A.7)$$

where $\Sigma_P = \int_0^d \sigma_P(z)\,dz$ is integral Pedersen conductivity. Since $\sigma_P = 0$ below and above the ionosphere, we have

$$j_\parallel(z = z_1) = j_\parallel(z = z_1 + d) = j_z/\sin\alpha.$$

If the characteristic horizontal scale of the disturbance l is sufficiently large and the angle α is not too close to zero, then the condition of thin ionosphere $l \gg d/\tan\alpha$ is satisfied. In this case Eq. (A.7) in the limit $d \to 0$ yields the boundary condition determining a jump of vertical electric field components at the transition through thin ionosphere coinciding with the plane $z = z_1$:

$$j_z(z_1 + 0) - j_z(z_1 - 0) = \Sigma_P\left(\frac{1}{\sin^2\alpha}\frac{\partial^2\varphi}{\partial x^2} + \frac{\partial^2\varphi}{\partial y^2}\right)\Big|_{z=z_1} \quad (A.8)$$

Another boundary condition in approximation of thin ionosphere is given by the potential continuity condition:

$$\varphi(z_1 + 0) - \varphi(z_1 - 0) = 0. \quad (A.9)$$

Condition (A.8) can be presented in the form of current continuity equation integrated through the ionosphere heights if to introduce the effective tensor of integral conductivity of the ionosphere:

$$j_z(z_1 + 0) - j_z(z_1 - 0) = -\nabla_\perp\cdot\mathbf{J}, \quad \mathbf{J} = \widehat{\underset{e}{\Sigma}}\,\mathbf{E}_\perp = -\widehat{\underset{e}{\Sigma}}\,\nabla_\perp\varphi,$$
$$\widehat{\underset{e}{\Sigma}} = \begin{pmatrix} \Sigma_P/\sin^2\alpha & \Sigma_H \\ -\Sigma_H & \Sigma_P \end{pmatrix}. \quad (A.10)$$

References

Afonin, V.V., Molchanov, O.A., Kodama, T., Hayakawa, M., Akentieva, O.A., 1999. Statistical study of ionospheric plasma response to seismic activity: search for reliable result from satellite observations. In: Hayakawa, M. (Ed.), Atmospheric and Ionospheric Electromagnetic Phenomena Associated with Earthquakes. Terra Scientific Publishing Company (TERRAPUB), Tokyo, p. 597.

Bilichenko, S.V., Inchin, A.S., Kim, E.F., Pokhotelov, V.A., Puschayev, P.P., Stanev, G.A., Streltsov, A.V., Chmyrev, V.M., 1990. Ultra low frequency response of the ionosphere to the process of earthquake preparation. Doklady Akademii Nauk SSSR (Doclady) 311, 1077–1081.

Borisov, N., Chmyrev, V., Rybachek, S., 2001. A new ionospheric mechanism of electromagnetic ELF precursors to earthquakes. Journal of Atmospheric and Solar-Terrestrial Physics 63, 3–10.

Burke, W.J., Aggson, T.L., Maynard, N.C., Hoegy, W.R., Hoffman, R.A., Candy, R.M., Leibrecht, C., Rodgers, E., 1992. Effects of a lightning discharge detected by the DE-2 satellite over Hurricane Debbie. Journal of Geophysical Research 97, 6359–6367.

Chmyrev, V.M., Isaev, N.V., Bilichenko, S.V., Stanev, G.A., 1989. Observation by space-borne detectors of electric fields and hydromagnetic waves in the ionosphere over an earthquake center. Physics of the Earth and Planetary Interiors 57, 110–114.

Chmyrev, V.M., Isaev, N.V., Serebryakova, O.N., Sorokin, V.M., Sobolev, Ya.P., 1997. Small-scale plasma inhomogeneities and correlated ELF emissions in the ionosphere over an earthquake region. Journal of Atmospheric and Solar-Terrestrial Physics 59, 967–973.

Gokhberg, M.B., Morgunov, V.A., Yoshino, T., Tomizawa, I., 1982. Experimental measurements of EM emissions possibly

related to earthquake in Japan. Journal of Geophysical Research 87, 7824–7827.

Holzworth, R.H., Kelley, M.S., Siefring, C.L., Hale, L.C., Mitchell, J.D., 1985. Electrical measurements in the atmosphere and the ionosphere over an active thunderstorm, 2. Direct current electric fields and conductivity. Journal of Geophysical Research 90, 9824–9831.

Isaev, N.V., Gdalevich, G.L., Benkova, N.P., 1987. Auroral electric field penetration into the middle-latitude trough. Advances in Space Research 7, 59.

Isaev, N.V., Sorokin, V.M., Chmyrev, V.M., Serebryakova, O.N., Ovcharenko, O.Ya., 2002a. Electric field enhancement in the ionosphere above tropical storm region. In: Hayakawa, M., Molchanov, O.A. (Eds.), Seismo Electromagnetics: Litosphere–Atmosphere–Ionosphere Coupling. TERRAPUB, Tokyo, pp. 313–315.

Isaev, N.V., Sorokin, V.M., Chmyrev, V.M., Serebryakova, O.N., Yaschenko, A.K., 2002b. Disturbance of the electric field in the ionosphere by sea storms and typhoons. Cosmic Research 40, 547–553.

Kelley, M.S., 1989. The Earth's Ionosphere: Plasma Physics and Electrodynamics, International Geophysical Series, vol. 43. Academic, San Diego, CA.

Kelley, M.S., Siefring, C.L., Pfaff, R.F., Kintner, P.M., Larsen, M., Green, M., Holzworth, R.H., Hale, L.C., Mitchell, J.D., Vine, D.I., 1985. Electrical measurements in the atmosphere and the ionosphere over an active thunderstorm, 1. Campaign overview and initial ionospheric results. Journal of Geophysical Research 90, 9815–9823.

Mikhailova, G., Mikhailov, Yu., Kapustina, O., 2000. ULF-VLF electric fields in the external ionosphere over powerful typhoons in Pacific oceans. International Journal of Geomagnetism and Aeronomy 2, 153–158.

Molchanov, O.A., Mazhaeva, O.A., Golyavin, A.N., Hayakava, M., 1993. Observation by the Intercosmos-24 satellite of ELF-VLF EM emissions associated with earthquakes. Annals of Geophysics 11, 431–440.

Park, C.G., Dejnakarintra, M., 1973. Penetration of thundercloud electric field into the ionosphere and magnetosphere. 1. Middle and subauroral latitudes. Journal of Geophysical Research 78, 6623–6633.

Parrot, M., 1994. Statistical study of ELF/VLF emissions recorded by a low-altitude satellite during seismic events. Journal of Geophysical Research 399, 23339–23347.

Phelps, A.D.R., Sagalyn, R.C., 1976. Plasma density irregularities in the high-latitude top side ionosphere. Journal of Geophysical Research 81, 515.

Raghavarao, R., Gupta, S.P., Sekar, R., Narayanan, R., Desai, J.N., Sridharan, R., Babu, V.V., Sudhakar, V., 1987. In situ measurements of winds, electric fields and electron densities at the onset of equatorial spread F. Journal of Atmospheric and Terrestrial Physics 49, 485.

Serebryakova, O.N., Bilichenko, S.V., Chmyrev, V.M., Parrot, M., Rauch, J.L., Lefeuvre, F., Pokhotelov, O.A., 1992. Electromagnetic ELF radiation from earthquake regions as observed by low altitude satellites. Geophysical Research Letters 19, 91–94.

Sorokin, V.M., Cherny, G.P., 1999. It is quite possible to monitor typhoons from outer space. Aerospace Courier (3), 84–87.

Sorokin, V., Yaschenko, A., 2000. Electric field disturbance in the Earth–ionosphere layer. Advances in Space Research 26, 1219–1223.

Sorokin, V.M., Chmyrev, V.M., Isaev, N.V., 1998. A generation model of small-scale geomagnetic field-aligned plasma inhomogeneities in the ionosphere. Journal of Atmospheric and Solar-Terrestrial Physics 60, 1331–1342.

Sorokin, V.M., Chmyrev, V.M., Hayakawa, M., 2000. The formation of ionosphere–magnetosphere ducts over the seismic zone. Planetary and Space Sciences 48, 175–180.

Sorokin, V.M., Chmyrev, V.M., Yaschenko, A.K., 2001. Electrodynamic model of the lower atmosphere and the ionosphere coupling. Journal of Atmospheric and Solar-Terrestrial Physics 63, 1681–1691.